TECHNICAL PAPER

ISSN:1047-3289 *J. Air & Waste Manage. Assoc.* **58**:879–890
DOI:10.3155/1047-3289.58.7.879

Characterization of Near-Road Pollutant Gradients Using Path-Integrated Optical Remote Sensing

Eben D. Thoma and Richard C. Shores
Office of Research and Development, National Risk Management Research Laboratory, Air Pollution Prevention and Control Division, U.S. Environmental Protection Agency, Research Triangle Park, NC

Vlad Isakov
National Oceanic and Atmospheric Administration, Sciences Modeling Division (In Partnership with U.S. Environmental Protection Agency), Research Triangle Park, NC

Richard W. Baldauf
Office of Research and Development, National Risk Management Research Laboratory, Air Pollution Prevention and Control Division, U.S. Environmental Protection Agency, Research Triangle Park, NC, and Office of Air and Radiation, Office of Transportation and Air Quality, National Vehicle and Fuel Emissions Laboratory, Ann Arbor, MI

ABSTRACT
Understanding motor vehicle emissions, near-roadway pollutant dispersion, and their potential impact to near-roadway populations is an area of growing environmental interest. As part of ongoing U.S. Environmental Protection Agency research in this area, a field study was conducted near Interstate 440 (I-440) in Raleigh, NC, in July and August of 2006. This paper presents a subset of measurements from the study focusing on nitric oxide (NO) concentrations near the roadway. Measurements of NO in this study were facilitated by the use of a novel path-integrated optical remote sensing technique called deep ultraviolet differential optical absorption spectroscopy (DUV-DOAS). This paper reviews the development and application of this measurement system. Time-resolved near-road NO concentrations are analyzed in conjunction with wind and traffic data to provide a picture of emissions and near-road dispersion for the study. Results show peak NO concentrations in the 150 ppb range during weekday morning rush hours with winds from the road accompanied by significantly lower afternoon and weekend concentrations. Traffic volume and wind direction are shown to be primary determinants of NO concentrations with turbulent diffusion and meandering accounting for significant near-road concentrations in off-wind conditions. The enhanced source capture performance of the open-path configuration allowed for robust comparisons of measured concentrations with a composite variable of traffic intensity coupled with wind transport (R^2 = 0.84) as well as investigations on the influence of wind direction on NO dilution near the roadway. The benefits of path-integrated measurements for assessing line source impacts and evaluating models is presented. The advantages of NO as a tracer compound, compared with nitrogen dioxide, for investigations of mobile source emissions and initial dispersion under crosswind conditions are also discussed.

IMPLICATIONS
NO is shown to be a useful tracer for characterization of mobile source emissions and dispersion in close proximity to major roadways. The DUV-DOAS system has proved to be a useful instrument for time-resolved measurement of NO in these applications. Near-road measurements using coordinated deployments of open-path systems, coupled with wind and traffic characterization, are shown to be useful tools for near-road impact studies.

INTRODUCTION
Mobile sources are ubiquitous and major contributors to U.S. air pollution emission inventories for criteria and air toxic pollutants.[1] A growing number of health studies have linked an increased occurrence of adverse health effects with proximity to heavily traveled roadways.[2–10] These health studies have focused on populations living, working, or going to school in the first several hundred meters of the road, where emissions from motor vehicles may not yet be fully diluted with background air. A large population is potentially at increased risk; over 35 million Americans have been estimated to live within 100 m of major transportation sources.[4,8,11] To address this emerging issue, the U.S. Environmental Protection Agency (EPA) has initiated a series of research studies to investigate traffic emission impacts on near-roadway environments, health implications, and potential mitigation strategies.[12]

In support of the EPA near-road research effort, this paper presents information on pollutant concentration and the initial stages of dispersion through characterization of nitric oxide (NO) levels in close proximity to a major highway as a function of wind and traffic conditions. These data represent a subset of measurements conducted near Interstate 440 (I-440) in Raleigh, NC, during a 2-wk measurement campaign in July and August 2006.[12] Data were acquired using a novel path-integrated optical measurement technique called deep ultraviolet differential optical absorption spectroscopy (DUV-DOAS) in conjunction with nitrogen oxide (NO_x) point monitors and advanced wind measurement and traffic characterization instruments.

NO as a Mobile Source Tracer

The concentration levels and dispersion of NO near roadways are important research topics because NO is the dominant component of primary NO_x emissions from most on-road vehicles[13] and its role in nitrogen dioxide (NO_2) formation and ozone chemistry is well known.[14] More importantly, NO can be useful as a surrogate to aid in understanding near-road emissions and dispersion because source discrimination capability is enhanced by NO's high near-road concentration compared with its low regional background levels. This is a distinct measurement advantage over other mobile source tracers such as NO_x, carbon monoxide (CO), and carbon dioxide (CO_2), which possess higher background concentrations. This practical measurement advantage is of clear importance for gaseous plume evolution studies and may help in understanding other mobile source pollutants. For example, Janhäll et al.[15] found that NO was a better tracer for mobile source-produced ultrafine particles than traffic intensity.

In particular, this study shows NO to be a more representative tracer of mobile source emissions compared with NO_2 under crosswind conditions. This is especially true for the morning rush hour period in which near-road pollutant concentrations are generally more pronounced because of lower boundary layers, comparatively calm wind conditions, and because atmospheric transformation potential of NO is generally less pronounced early in the day. Although this work focuses on NO characterization using coordinated path-integrated optical measurements, the relative utility of NO as a tracer is demonstrated though a comparison of point monitor measurements of NO_x, NO, and NO_2 concentrations at different distances from the road. This point carries special importance because NO_2 has been traditionally used as a tracer for near-road impact studies and may be of limited usefulness when examining short-term effects in close proximity to the roadway.

NO Measurement Using ORS

As part of the overall effort to increase understanding of the spatial and temporal distribution of air pollutants in near-road environments, EPA is extending its use of optical remote sensing techniques developed for area source measurement[16–18] to assess mobile source emissions and pollutant dispersion. Ground-based ORS instruments utilize infrared (IR), visible, or ultraviolet (UV) light beams projected over extended distances to spectroscopically sample the intersected air column, producing an average concentration measurement of the gaseous pollutants of interest. ORS techniques possess several advantages over traditional point sampling techniques with regard to the assessment of inhomogeneous extended area sources. Open-path instruments produce a path-averaged concentration (PAC) measurement, providing a more representative sample of average emissions from spatiotemporally variable sources. ORS techniques directly sample the intersected air mass, providing a near real-time in situ measurement. The projected optical beams utilized in ORS can be directed along multiple paths, allowing for vertical and horizontal concentration gradient assessment from a single directionally scanned instrument or multiple instruments in coordinated deployment. Taken together, these factors provide for enhanced capability for assessments of line source impacts and evaluations of roadway emission and dispersion models. These advantages are discussed in this work, which examines coordinated acquisition of path-integrated NO concentration data along two sampling paths deployed parallel to the roadway.

A disadvantage of ORS systems lies in the fact that minimum quantification limits are modest in comparison with time-integrated sampling techniques. With few exceptions, near-road pollutant concentrations are generally below the quantification limit for open-path tunable diode laser and open-path Fourier transform IR (OP-FTIR) instrumentation currently utilized by EPA for area source measurements.[17,19] To help address this issue, EPA is investigating use of deep UV differential optical absorption spectroscopy (DUV-DOAS) with improved detection limits for mobile source pollutants. One objective of this work is to describe the development and use of DUV-DOAS for time-resolved NO characterization in near-road environments.

METHODOLOGY

Description of DUV-DOAS Instrument

Open-path UV spectroscopy has previously been used for mobile source emission research in two ways: (1) single vehicle remote tailpipe emission measurements, and (2) long-path air quality monitoring near roadways. Single vehicle remote sensing techniques utilize a crossroad optical path that intersects the emission plume of the passing vehicle and have been used to assess fleetwide emission factors and the impact of high-emitting vehicles.[20–24] Commercial crossroad remote sensing systems are portable, robust, and produce highly time-resolved data (<1 sec), but are generally limited in compound speciation and detection limit capabilities. Additionally, crossroad measurements represent a moment in time in close proximity to the tailpipe, limiting their usefulness for dispersion and exposure studies. Long-path UV-DOAS systems for air quality monitoring utilizing optical path lengths in the 200-m to 2-km range are well developed and have been applied in several mobile source-related studies.[25–29] Long-path UV-DOAS systems usually possess lower time resolution (1–5 min) but enhanced detection and discrimination capability compared with crossroad systems. Long-path systems are generally less portable and require significant site infrastructure for successful operation. The system discussed here shares aspects of both measurement approaches, being designed for parallel roadway deployments with approximate 150-m path lengths and time resolutions on the order of a few seconds. The DUV-DOAS system described is portable and robust, with measurement performance somewhere in between the cross-road and long-path approaches.

Hardware Description

The DUV-DOAS system used for this work is a modified version of the UV Sentry system manufactured by Cerex Environmental Services. The DUV-DOAS instrument consists of a separate UV light source and receiver, each fitted with 6-in. collimating and receiving reflective mirror optics. The source utilizes a 30-W deuterium lamp with effective output starting at approximately 190 nm. The receiver houses a temperature-stabilized, fiber-coupled broad-band 2048 element diode array spectrometer with a data point spacing of approximately 0.076 nm. The spectrometer is powered and controlled via a USB connection to the control computer. The control computer is a standard PC with Windows XP operating system and Cerex control software. The prototype DUV-DOAS is configured for deep UV operation through proprietary selection of optical coatings and lamp by Cerex Environmental Services.

To illustrate the deep UV performance of the prototype, it is informative to compare the operational spectral range of several DOAS configurations. Figure 1a shows normalized spectral intensities for a continuous output xenon lamp standard in long-path DOAS applications (trace 1), a UV-optimized continuous output xenon using a UV pass filter (trace 2), a standard UV Sentry deuterium system (trace 3), and a DUV system (trace 4). Additional signal in the 200- to 220-nm range is evident for the DUV-DOAS prototype. Figure 1b (trace 1) shows an optical absorption spectrum for NO acquired with the DUV-DOAS system. From a spectral range standpoint, the DUV prototype is capable of resolving the 204.5-nm NO absorption peak and above. Measurements for this work utilize the 214.8-nm spectral feature.

NO Analysis Software

To derive the concentration of NO from the DUV spectral data, a Matlab-based fitting routine was developed by EPA. The path-integrated concentration (PIC) of NO is calculated by a least-squares fit of a 3.5 parts per million meter (ppm·m) NO reference spectrum to the field absorbance spectrum created using a low NO background. The technique uses second derivative Savitzky–Golay filter processing of the absorbance spectra to isolate the sharp NO spectral features from broad-band absorptions and time-varying baselines.[30,31] Figure 1b illustrates this point by comparing a 1-m path length, 14 ppm by volume NO absorption spectrum (trace 1) with the same spectrum processed with a second derivative, third order polynomial fit, 25 frame Savitzky–Golay filter (trace 2). The Savitzky–Golay traces have been multiplied by a factor of 30 for ease of viewing. The NO absorption feature in trace 1 is superimposed on a variable baseline that is significantly above zero in the analysis region and below zero at 240 nm and above. Spectral features that exhibit slow wavelength-dependent variations are effectively decoupled from the sharp NO absorption features by the second derivative analysis technique as evidenced in the flat baseline of trace 2. This is important for near-road measurements because baseline variations caused by broadband hydrocarbon absorptions are frequently observed. It is also noted that the Savitzky–Golay filtering techniques reduce high-frequency noise and can be optimized through choice of filter characteristics to enhance various spectral features of interest as part of this modified DOAS analysis approach.

Calibration for NO

The current work utilized two time-synchronized DUV-DOAS systems in coordinated deployment to assess small differences in NO concentrations, requiring particular attention to be paid to inter-unit comparability. NO measurement performance was evaluated using a large aperture open-path calibration cell designed for insertion into the beam path without significant loss in optical power. The cell consists of a 1-m long, 20-cm diameter stainless steel cylinder fitted with 20-cm diameter, 0.32-cm thick S1 grade quartz windows secured by steel rings and polytetrafluoroethylene gaskets. The cell is designed for flow-through operation of a calibration gas mixture. For calibration and comparison trials, a 29.8-ppm NO ($\pm$2.5%)

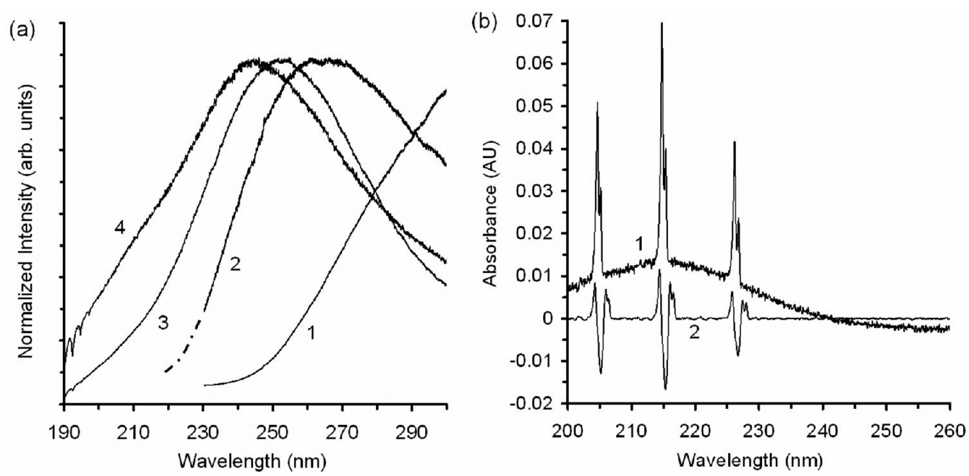

Figure 1. (a) Normalized spectral intensities of typical UV DOAS configurations. (b) Comparison of NO absorbance spectra with (1) no Savitzky–Golay processing and (2) with Savitzky–Golay processing.

in-balance nitrogen gas supply was diluted to test levels with ultrahigh purity nitrogen using a calibrated gas dilution system (Series 2000 Environics).

Figure 2 shows a NO measurement response comparison between two similarly configured DUV-DOAS systems (unit 1 and 2) used in the near-roadway field study subsequently described. The systems were set up using 10-m separations between the source and receiver with optical paths crossed at the midpoint, allowing the centrally located open-path cell to be accessed by each beam path in sequential fashion. The open-path cell was filled to a concentration set point and each unit quantified the NO concentration before moving to the next point. The integration time for each calibration data point was 5 sec, and the system was allowed to stabilize before acquiring data at each concentration level. It is evident from Figure 2 that the two systems are in close agreement over an operational range encountered in this field study.

In typical field operation, the tripod-mounted DUV-DOAS system exhibits acceptable performance for optical path lengths up to approximately 200 m. At greater distances, low signal strength and source-to-receiver optical alignment drift become problematic. For near-road studies, the 214.8-nm spectral feature for NO analysis is believed to be free of interfering atmospheric species. To ensure low interference impact potential, a relatively conservative analysis fit value limit of 0.7 R^2 was imposed, leading to an effective minimum quantification limit of 7 ppb.[30]

Equipment Configuration for Near-Roadway Measurements

As shown in Figure 3, two DUV-DOAS systems were configured adjacent to I-440 in Raleigh, NC, with 149-m optical beam paths parallel to the highway at distances of 7 m (unit 1) and 17 m (unit 2) from the edge of the nearest travel lane. The optical beam paths were 2 m above road level. The DUV-DOAS systems operated over an approximate 14-hr time period each day starting before the morning rush hour and ending after the peak of the evening

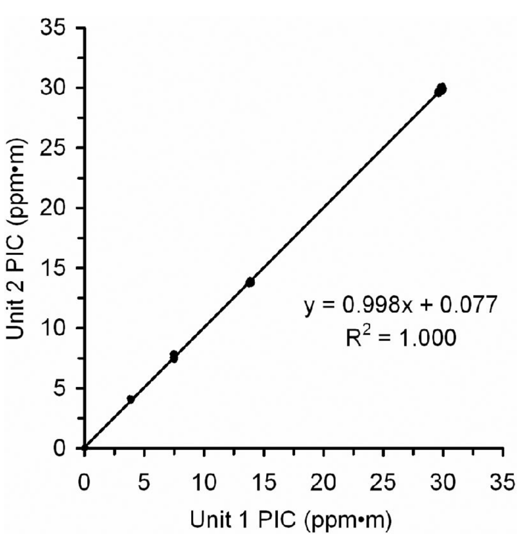

Figure 2. Comparison of NO PIC measurement response of two DUV-DOAS systems used for Raleigh near-road field study (n = 444).

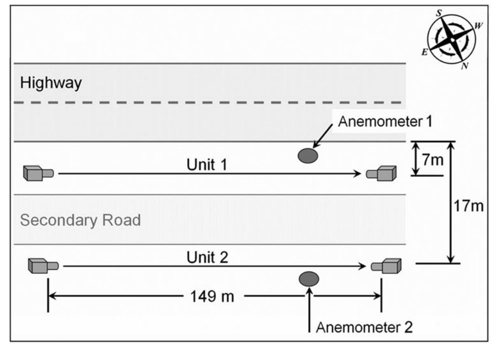

Figure 3. Schematic map of field experiment with configuration of DUV-DOAS systems and location of sonic anemometer.

rush hour (typically 5:00 a.m. to 7:00 p.m.). Measurements were performed on 9 weekdays and 4 weekend days during the study. The DUV-DOAS systems utilized a 5-sec signal integration time with system timing actively synchronized with wind measurements using clock control software (Beagle Software, Inc.).

Near-road wind data were acquired with two Model 81000 sonic anemometers (R.M. Young Co.) operating at a 4-Hz data acquisition rate. One anemometer (Sonic-5) was located in close proximity to the optical path of unit 1, as indicated in Figure 3, at a height of 2 m above ground level and 5 m from the travel lane. A second unit (Sonic-20) was located near the optical path of unit 2, approximately 20 m from the roadway at 8 m above ground level. For combined NO_x, NO, and NO_2 measurements, two chemiluminescent analyzers were deployed in sampling trailers located 20 m from the roadway (API 200A, Teledyne Instruments) in close proximity to the optical path of unit 2 and 300 m from the roadway (Thermo Electron Model 42S). Data from the NO_x analyzers are presented here primarily in support of the open-path measurements.

Vehicle class-resolved traffic measurements were made with a traffic camera and subsequent analysis using the automated Tigereye traffic count software (DTS Inc.). Traffic counts were performed in 20-sec time blocks with car and heavy trucks separately logged. Additionally, CO PAC data from an open-path FTIR (IMACC Inc.), deployed parallel and adjacent to the unit 2 DUV-DOAS 16 m from the roadway, provide supporting data for this report.[12]

I-440 is an eight-lane highway, approximately 32 m wide, which carries a daily weekday traffic volume of approximately 125,000 vehicles (average 4% heavy-duty trucks) during the study. Highway traffic experienced varying operating conditions, from congestion to free flowing at approximately 50–60 mph. A lightly traveled secondary road (≈200 vehicles per day) was parallel to and between the unit 1 and 2 optical paths. The secondary road had a large proportion of heavy diesel traffic (≈25%), partially in acceleration mode because of a speed bump near the field site (≈30 mph average speed). The orientation of the highway source was from 116 to 296° from the north, as indicated in Figure 3. A wind direction of 206° corresponds to conditions when winds blow directly from the highway towards the optical paths. Weather conditions for the study were typical for summer in Raleigh, NC, with strong sunshine, high relative humidity, and afternoon temperatures reaching into the low to mid 90s. Discussions on general field study characteristics, including the site descriptions, study meteorology summaries, and instrumentation/monitoring strategies are described in a companion methods paper.[12]

RESULTS AND DISCUSSION

Time-Resolved NO Measurements

Figure 4 shows typical 5-sec time-resolved DUV-DOAS NO PAC data for the study in ppb by volume. Figure 4a shows a complete daily dataset, whereas Figure 4b shows an expanded temporal view of the same data. This figure illustrates three typical aspects of the study data: (1) NO concentrations reached a peak during the morning rush hour period, with concentrations in the 150-ppb range under heavy traffic load with winds from the roadway; (2) NO concentrations on the 7-m path (unit 1) were higher than on the 17-m path (unit 2); and (3) the temporal variability in the 5-sec time regime was large, with discernable short time-duration spikes in NO concentrations. The temporal variability in NO concentration is more clearly seen in Figure 4b, which shows results on an expanded time scale at the beginning of the morning rush hour period. This temporal variability is attributed to discrete emissions of vehicles traversing the path, coupled with observed highly variable winds influenced by traffic-induced turbulence. The degree of temporal correlation between unit 1 and unit 2 evident in Figure 4b is typical for the entire study.

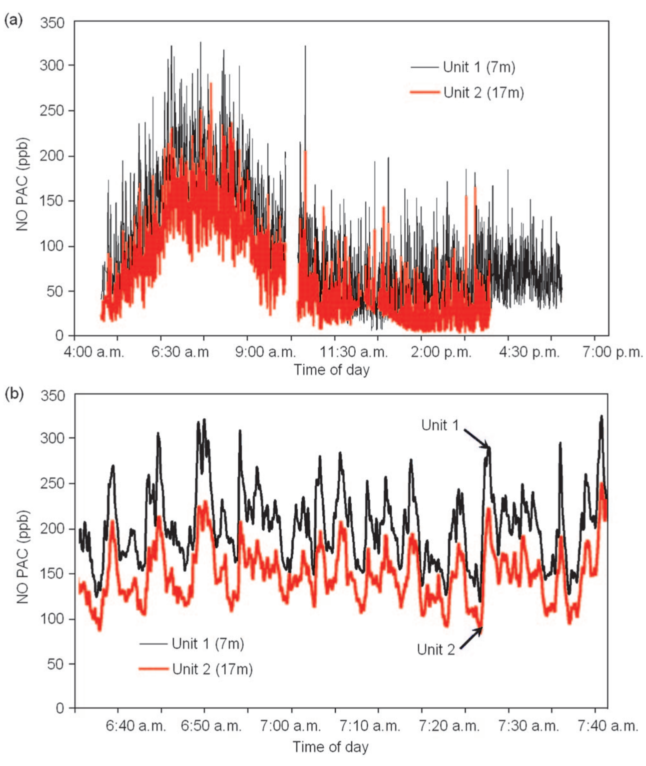

Figure 4. NO PAC at 5-sec time resolution: (a) during one day of measurements on Friday, July 28, 2006; and (b) and expanded version of same data at the beginning of rush hour on Friday, July 28, 2006.

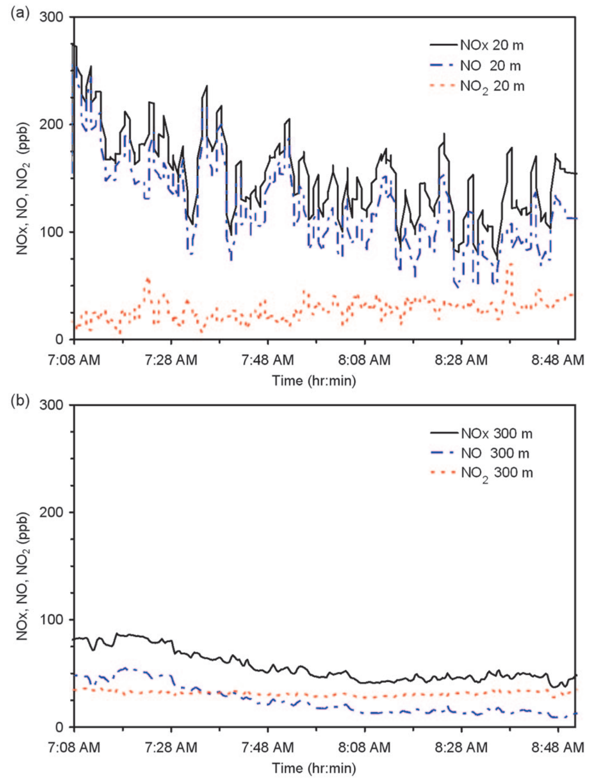

Figure 5. Measurements of NO_x, NO, and NO_2 at (a) 20 m and (b) 300 m from the roadway during a typical weekday morning rush hour with winds from the roadway.

The comparative utility of NO as a tracer for mobile source emissions is demonstrated in Figure 5, which shows the relative variation in NO, NO_2, and NO_x concentrations at 20 and 300 m from the roadway during a typical weekday morning rush hour (Thursday, August 3) with stable winds directionally from the road measured with 20-sec time resolution. Figure 5a shows that the total NO_x signal at 20 m is dominated by NO, with a much weaker NO_2 signature. Simultaneously, at the 300-m site (Figure 5B) NO_x and NO concentrations are significantly lower, with NO showing a more pronounced relative decrease. NO_2 concentrations at the 300-m site are similar to but slightly elevated compared with the NO_2 measured at the 20-m site, implying some atmospheric conversion of NO over the plume transit distance. The variability in NO_x and NO signal at 20 m is similar to that portrayed in Figure 4 and is caused by the close proximity of the source. The NO_2 signal at 20 m shows less temporal variability and likely reflects a composite of temporally stable regional background, with a weak contribution from the source. This figure suggests that NO_2 measurements represent impacts from regional sources rather than impacts from primary vehicle emissions for these conditions. This analysis suggests that NO is a preferable mobile source tracer compared with NO_2 for measurement studies conducted in close proximity to the roadway, particularly during the important morning rush hour time periods under crosswind conditions. An analysis of the relative contribution of NO and NO_2 to near-road NO_x for periods throughout the day is addressed in a subsequent section.

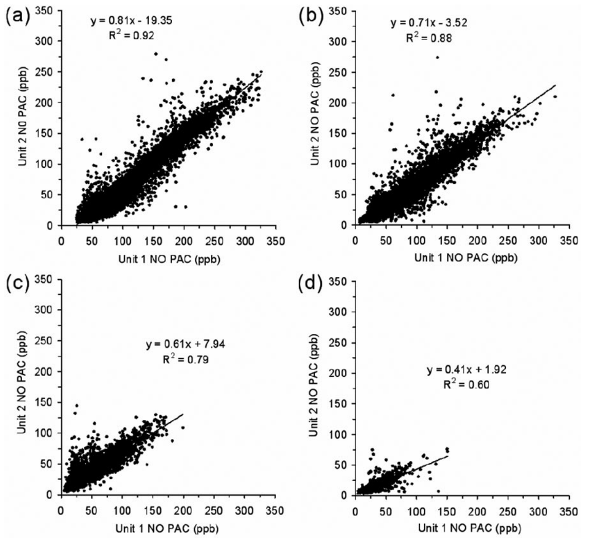

Figure 6. Comparison of units 1 and 2 5-sec NO concentration data for (a) Friday, July 28, (b) Monday, August 7, (c) Saturday, July 29, and (d) Sunday, August 6, 2006 ($n > 5000$).

For studies investigating the initial dispersion of pollutants near the roadway, effective capture of the plume is important. Path-integrated measurements provide an advantage over point monitors in this regard because their spatially extended sampling nature yields a higher probability that codeployed instruments will similarly intersect the evolving plume. Sufficient measurement time-resolution is additionally important for robust characterization of temporally variable sources in turbulent transport environments such as that encountered near roadways. The parallel 149-m open-path configuration of the DUV-DOAS systems operating at 5-sec time resolution demonstrates both of these advantages. This is evidenced by the generally good point-by-point correlations of 5-sec NO PAC data from the DUV-DOAS systems shown in Figure 6 for four different days of observations: (a) Friday, July 28, (b) Monday, August 7, (c) Saturday, July 29, and (d) Sunday, August 6, 2006. The selected dates represent different types of observed traffic and meteorological conditions: heavy traffic during weekdays (Figure 6, a and b), low traffic during weekends (Figure 6, c and d), winds mainly from the road (Figure 6, a and c), and not always from the road (Figure 6, b and d). Correlation slope factors for individual days are dependent upon mean daily wind directions, with values approaching a minimum of 20–30% for days having a significant number of time periods with winds predominately from the road. Detailed in a later section, the percentage difference in NO PAC between unit 1 (7 m) and unit 2 (17 m) depends on the wind direction, which is not constant throughout the day. This variability in wind direction partially accounts for the width of the correlation bands around the regression lines in Figure 6. The few observed outliers are ascribed primarily to traffic on the secondary road, which can exhibit a disproportionate impact to the NO concentrations measured on a given side because of the optical path arrangement that straddles the source (Figure 3). For Figures 4 and 6, a temporal shift of 10 sec has been applied to unit 2 to compensate for the average transit time of the plume, which was around 1 m/sec for most observation periods. A 10-sec temporal shift produced the best overall correlation in these daily datasets within the resolution of the measurement at 5 sec per sample.

Time-Averaged NO Concentrations, Traffic Counts, and Meteorology

Time-resolved observations reveal a wide range of variability in NO concentrations. To eliminate the effect of short-time duration spikes to facilitate investigations of wind and traffic influence, we computed time-averaged NO concentrations, traffic, and meteorology. Figures 7 and 8 present examples of 10-min moving average data from Thursday, August 3 and Wednesday, August 9, respectively. Figures 7a and 8a summarize NO PAC data in ppb (primary ordinate axis) and traffic data in counts per 20 sec (secondary ordinate axis), whereas Figures 7b and 8b present wind direction in degrees from true north (primary ordinate axis) and horizontal wind speed in m/sec (secondary ordinate axis). The shaded areas represent wind data graphs from 170 to 240° to aid in visualization of wind directions generally from the highway with significant projections onto the 206° normal vector.

Figure 7a shows that NO concentrations strongly peak in the 6:00 to 8:00 a.m. morning rush hour time frame. This is the typical observed NO concentration behavior for weekdays during this study. The peak in NO

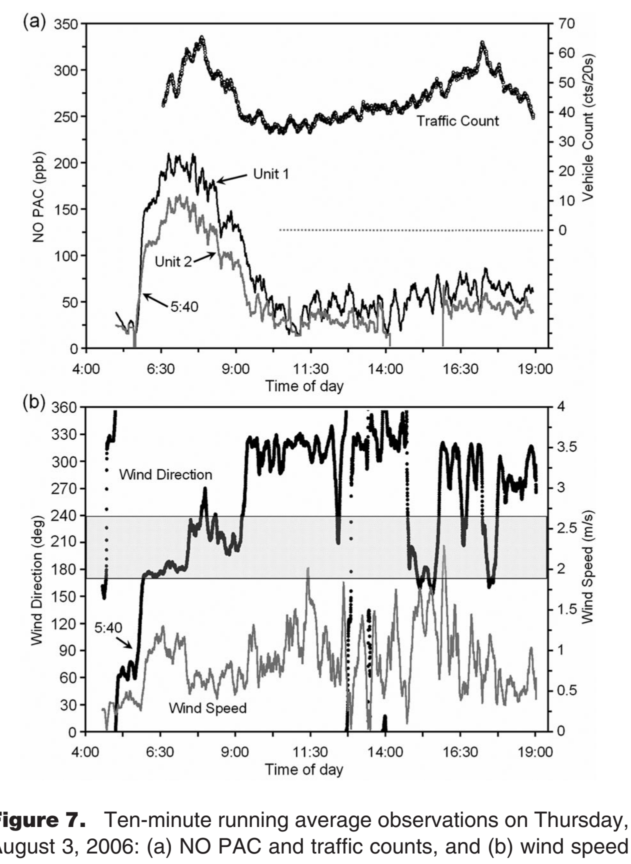

Figure 7. Ten-minute running average observations on Thursday, August 3, 2006: (a) NO PAC and traffic counts, and (b) wind speed and direction.

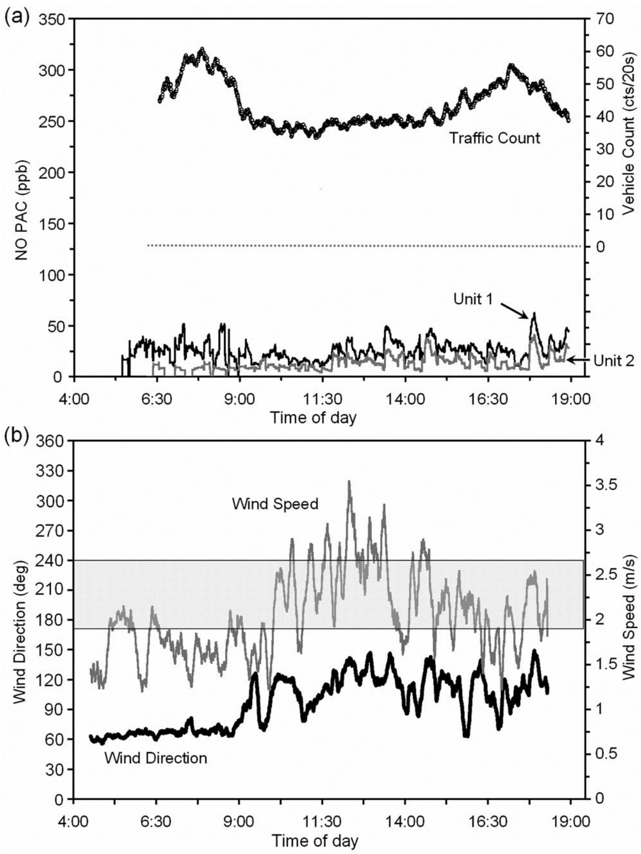

Figure 8. Ten-minute running average observations on Wednesday, August 9, 2006: (a) NO PAC and traffic counts, and (b) wind speed and direction.

concentration in Figure 7a corresponds with a combination of high traffic volume and near-normal winds (bearings around 206°) occurring during this time frame (Figure 7b). Note the rapid onset of high NO concentration coincident with wind vector change at 5:40 a.m. The concentration of NO is reduced around 9:00 a.m., coincident with lower traffic volume, and a change in wind direction and the NO PAC remains relatively low for the remainder of the day. Comparably lower NO concentrations observed during the evening rush hour are typical for all weekday data acquired during this study. Note that wind speeds are relatively low, in the 1-m/sec range, with a higher degree of variability in the afternoon.

As a contrast, Figure 8, a and b, shows data from Wednesday, August 9 under wind conditions directionally away from the road, consequently resulting in low measured NO PAC values for the entire day. Note that significant NO concentrations are observed even when the 10-min average wind direction is outside of the shaded region from 170 to 240° (i.e., when the wind is not blowing directly from the source). During these time periods NO concentrations measured at the 300-m site were in the 1-ppb range, far below those observed near the road, indicating that regional sources are probably not responsible for the observed concentrations. The observed near-road concentrations are likely due to the effect of meandering of emissions from the roadway source, caused in part by traffic-driven turbulence and are discussed further in a later section. The observation of significant pollutant concentrations when winds are not directionally from the road is important for near-road studies because receptors can exist in unusually close proximity (<100 m) to the source.

Diurnal Variability in NO_x, Traffic, and Meteorology

Crossday Average NO and NO_x Concentrations. To help relate observed NO concentrations to traffic volume and wind conditions, we analyzed these parameters as a function of hour of day for the entire study. Figure 9, a and b, shows the variability of hourly average NO concentration data for weekdays and weekend days, respectively. In addition to the NO PAC data from the DUV-DOAS systems, NO concentration data from an API NO_x analyzer stationed 20 m from the travel lane near the unit 2 path are also presented. As discussed previously, the characteristic high NO concentrations during the weekday morning rush hour are evident in Figure 9a. It is noted that only 1 of 9 weekdays failed to show evaluated morning rush hour concentrations, Wednesday, August 9, with winds strongly away from the road. The reduced NO concentrations observed by the DUV-DOAS systems during the afternoon and evening rush hour time periods are confirmed by the API 200A readings. It is evident that weekend NO levels were much lower than weekday values

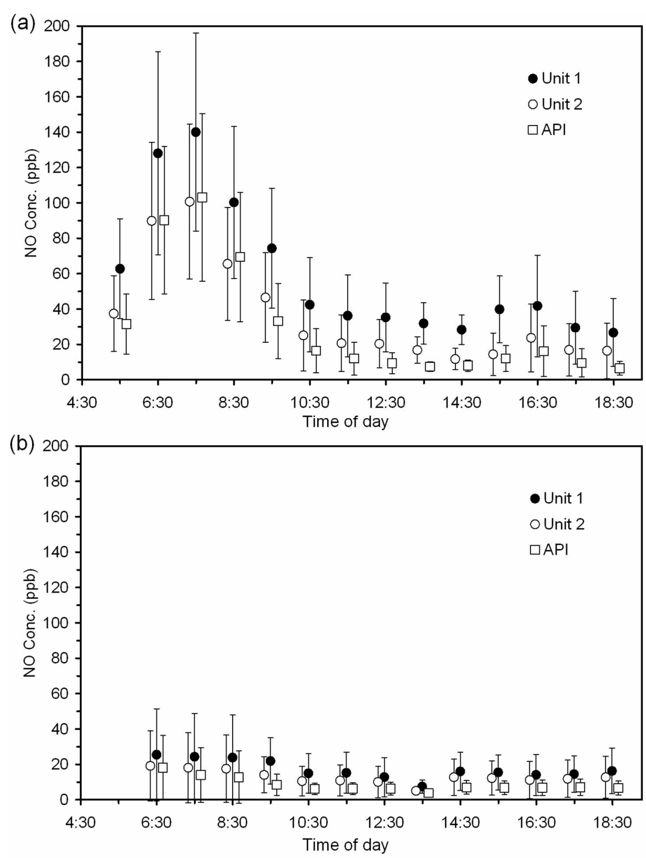

Figure 9. Hourly NO concentrations from unit 1 and 2 DUV DOAS compared with API 200A NO_x analyzer: (a) for all weekday measurements, and (b) for all weekend measurements.

Table 1. Hourly averages for 9 weekday measurements.

Hour Midpoint	Unit 1 NO PAC (ppb)	Unit 1 SD (ppb)	Unit 2 NO PAC (ppb)	Unit 2 SD (ppb)	Traffic (counts/20 sec)	Wind Direction (degrees)
5:30 a.m.	65.3	26.6	38.7	19.8		138.7
6:30 a.m.	139.2	50.6	97.2	39.3	36.0	164.0
7:30 a.m.	149.8	53.0	108.6	41.8	52.5	176.2
8:30 a.m.	109.2	46.0	73.2	36.1	44.9	191.3
9:30 a.m.	78.9	35.6	49.0	26.7	34.3	187.3
10:30 a.m.	52.1	31.0	30.2	20.6	30.4	201.9
11:30 a.m.	42.2	23.0	23.6	14.7	33.8	279.3
12:30 p.m.	37.8	17.4	20.1	12.0	36.7	318.0
1:30 p.m.	36.3	13.0	18.4	7.2	36.6	332.9
2:30 p.m.	36.6	14.9	16.9	9.9	39.0	328.4
3:30 p.m.	41.5	18.4	16.9	11.2	42.7	344.8
4:30 p.m.	44.6	26.3	20.1	17.7	49.6	326.2
5:30 p.m.	39.3	22.2	16.7	14.3	48.2	323.3
6:30 p.m.	35.6	20.2	16.9	15.3	38.1	324.0
Average	64.9	28.5	39.0	20.5		

for this study. This is explained by a combination of lower traffic volumes and variable winds, which were primarily away from the road during the weekend observation times (Tables 1 and 2). The error bars indicate ± 1 standard deviation in the hourly results. The API readings compare favorably with the proximate unit 2 results. The API instrument and unit 2 agree less well at low NO concentrations, primarily because of a higher number of nondetects for the API 200A, which are caused in part by the point sampling nature of the API as compared with the extended-path sampling offered by the DUV-DOAS. For this comparison, substituted values of 3.65 and 3.50 ppb were used for nondetect readings for the API (below 7.3 ppb) and unit 2 (below 0.7 R^2 fit value),[30] respectively. Figure 9 reflects a subset of available data when all instruments were in operation simultaneously. The overall hourly average data completeness percentage for units 1 and 2 was 100 and 98.3%, respectively, whereas the API unit completeness percentage was 78.5% of 177 possible hourly readings. The primary nonoperation cause for the API was related to overheating (air conditioning issues) on extreme temperature days (>95°F). The primary nonoperation cause for the DUV-DOAS systems was loss in optical alignment. The significantly greater operation time exhibited by the DUV-DOAS systems is an indication of their operational robustness.

It was shown previously in Figure 5 that NO accounts for a large percentage of the NO_x signal for the morning rush hour time periods in this study. In a similar fashion to Figure 9a, it is instructive to investigate the hourly average NO_x concentrations and relative contributions of NO and NO_2 for all weekdays of the study in conjunction with average CO values. Figure 10 presents these data as determined by the API chemiluminescent analyzer at the 20-m location, along with CO PAC data from an open-path FTIR located at 16 m.

It is evident from Figure 10 that NO contributes the majority of the NO_x signal during the weekday morning rush hour time periods and that the overall NO_x signal is lower in the afternoon. The NO_2 signal remains relatively

Table 2. Hourly averages for 4 weekend day measurements.

Hour Midpoint	Unit 1 NO PAC (ppb)	Unit 1 SD (ppb)	Unit 2 NO PAC (ppb)	Unit 2 SD (ppb)	Traffic (counts/20 sec)	Wind Direction (degrees)
6:30 a.m.	25.4	26.1	19.1	19.9	8.1	78.3
7:30 a.m.	24.3	24.3	18.1	19.8	9.9	52.3
8:30 a.m.	23.8	24.1	17.5	19.0	11.7	56.5
9:30 a.m.	21.8	13.2	14.0	10.2	15.6	34.6
10:30 a.m.	14.9	11.2	10.5	8.3	18.9	62.8
11:30 a.m.	13.4	10.6	9.5	7.9	19.4	96.6
12:30 p.m.	12.8	9.6	9.4	7.7	21.8	106.5
1:30 p.m.	11.5	8.2	9.2	7.8	21.4	104.8
2:30 p.m.	13.6	10.2	10.6	9.5	23.5	88.4
3:30 p.m.	12.6	9.9	10.0	9.2	26.5	87.1
4:30 p.m.	12.0	10.6	9.4	9.7	24.3	80.9
5:30 p.m.	12.5	9.5	9.9	9.8	23.2	87.2
6:30 p.m.	13.8	12.0	10.5	11.0	24.0	103.6
Average	16.4	13.8	12.1	11.5		

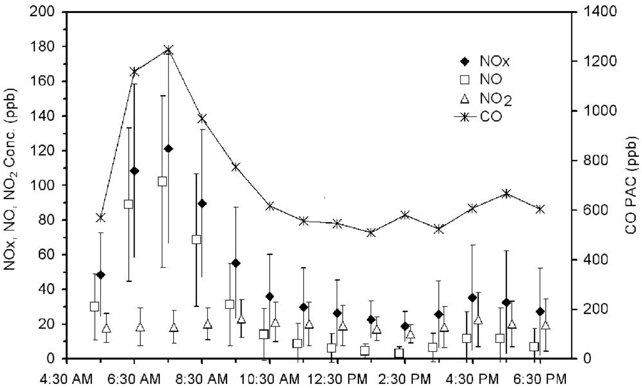

Figure 10. Hourly average concentrations of NO_x, NO, and NO_2 from the API NO_x analyzer and CO concentrations from open-path FTIR at the 20-m location for all weekdays.

constant throughout the day, similar to background levels. This indicates that it is unlikely that the lower afternoon NO concentrations presented in Figure 9 are caused by enhanced atmospheric conversion to NO_2 in the afternoon at the near-road observation points for this study. The CO trace of Figure 10 shows a similar temporal profile to NO_x, with comparatively low evening rush hour concentrations implying a roughly similar emission profile. Figures 9 and 10 suggest that other factors, such as changes in wind direction and enhanced afternoon dispersion, likely account for the reduced evening rush hour concentrations. It is noted that NO_x concentrations for weekend days are lower, similar to Figure 9b, with relative contributions similar to Figure 10. Figure 10 includes all native measurements produced by the API NO_x analyzer, which includes a significant number of readings below the average minimum detection limit of 7.3 ppb, accounting for the slightly lower NO levels compared with Figure 9.

Crossday Average Wind and Traffic Data. Differences in weekday morning and evening rush hour concentrations are further explored in Figure 11, which presents distributions of 10-min average wind directions from the sonic anemometers at 5 and 20 m (Figure 11a) and mean and standard deviations of traffic counts (Figure 11b) as a function of hour of day for all weekdays during the study. Figure 11b indicates weekday evening rush hour traffic volumes were similar to morning rush periods, arguing against reduced source levels as the cause for lower observed afternoon NO concentrations. Figure 11a shows winds during morning rush hours were generally from the road (strong overlap with the 206° normal vector) whereas afternoon winds were more variable and often parallel or away from the road. This diurnal wind pattern indicates that less effective wind transport is likely the most significant factor in the observed differences between morning and afternoon rush hour measured NO concentrations. The box symbols of Figure 11a represent the 25–75th percentile range, whereas the vertical bars indicate the 5–95th percentile range. Note that results from 20 m at 8 m above the ground differ slightly from the 5-m sonic readings, indicating possible influence from traffic-driven turbulence. This effect is further discussed in following sections.

Hourly average NO concentrations, traffic counts, and wind direction from the 5-m sonic readings are summarized in Tables 1 and 2 for all weekday and weekend observations, respectively. It is noted that the overall weekday hourly average NO concentration (64.9 ppb) is a factor of 4 higher than the similar weekend value (16.4 ppb). Although reduced weekend NO concentrations are expected because of lower traffic volume, this difference is exaggerated, due in large part to weekend wind directions being primarily away from the road during this study.

Correlation of NO PAC with Traffic and Wind Transport

The degree to which near-road NO concentrations are determined by traffic and effective wind transport is explored in Figure 12, which compares unit 1 NO PAC with a composite variable of traffic intensity multiplied by a time-weighted wind vector projection. The time-weighted wind projection approximately accounts for the short time-scale transport to the near-road measuring locations by defining 5-sec wind direction averaging subperiods within the 30-min observation period. All positive wind vector projections onto the 206° normal vector for a given 30-min period are summed and the result is weighted by the percentage of total possible positive projections (fraction of 360). This approximates a wind transport function for the 30-min observation period. Each data point in Figure 12 represents an average of 30-min periods binned

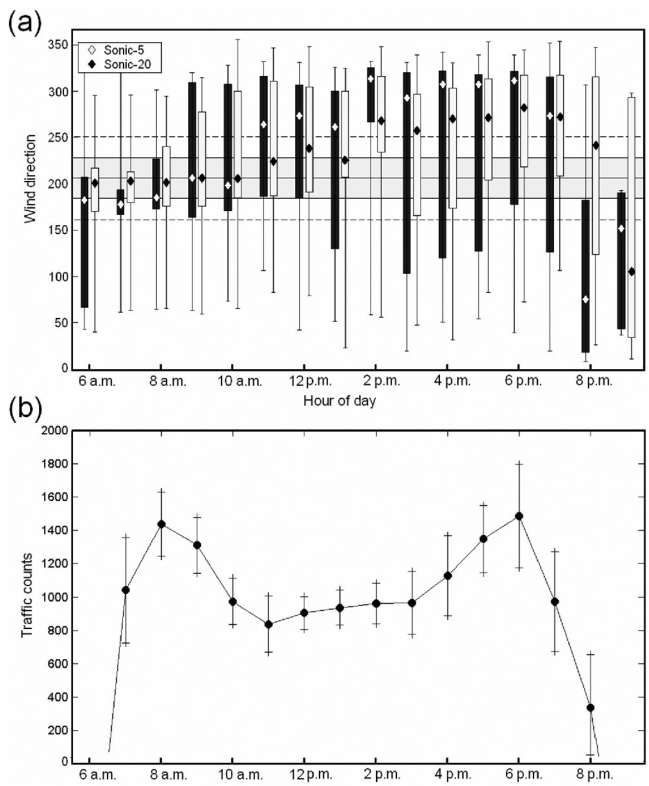

Figure 11. Diurnal distributions of (a) wind direction and (b) traffic counts (number of cars per 10-min intervals) for all weekdays. Box symbols in panel (a) represent 25–75th percentile range, whereas the vertical bars indicate 5–95th percentile range. Vertical bars in panel (b) indicate 1 standard deviation range.

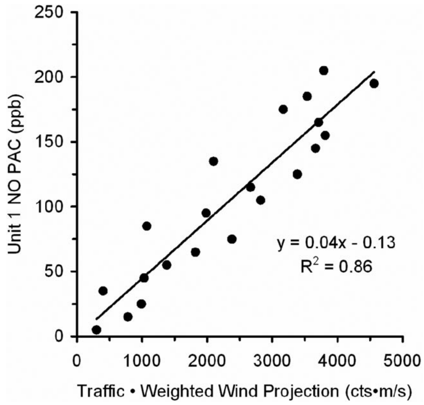

Figure 12. NO PAC measured by unit 1 (7 m from road edge) vs. time-weighted wind vector normal projection multiplied by total vehicle counts over a 30-min period.

by NO PAC values in 10-ppb intervals. The evident correlation between the measured concentrations and the product of traffic and weighted wind projection indicates a robust capture of the source by the open-path measurement and points to future possibilities of emission characterization utilizing the parallel experimental configuration.

Effects of Near-Road Turbulence

A time-weighted projection is utilized in Figure 12, because as discussed in Figures 7 and 8, significant NO PACs were measured close to the roadway even when time-averaged wind directions were away from the road. This is a consequence of the high degree of variability in wind direction due in part to traffic-driven turbulence affecting the near-road observing locations. This is a potentially significant effect when considering the impact of mobile source-generated pollution to near-road populations that can exist in close proximity to the source. This effect is examined here in a preliminary fashion by considering the disorganized transport by complex flows next to the source to be upwind meandering.[32] To understand the relative impact of meandering, it is useful to examine the mean and turbulent velocities, wind speed, and direction as measured at the 5- and 20-m sites. The distributions of vertical and horizontal turbulent intensities (σ_v/U and σ_w/U, respectively) are shown in Figure 13 as a function of hour of day for all days of observation. The diurnal behavior of vertical and horizontal turbulent intensities was similar to that of the wind speed, with the lower values occurring during the morning and the higher values occurring during the afternoon.

The vertical turbulent intensity varied from 0.1 to 1 during the course of the day, with large values exceeding 1.5 occurring between 12:00 and 5:00 p.m. The majority of the horizontal turbulent intensities were between 0.2 and 0.6. The meteorological observations indicated that turbulence near the road was significant, therefore, both direct transport by the mean wind and turbulent diffusion likely impacted pollutant concentrations and dispersion near the road.

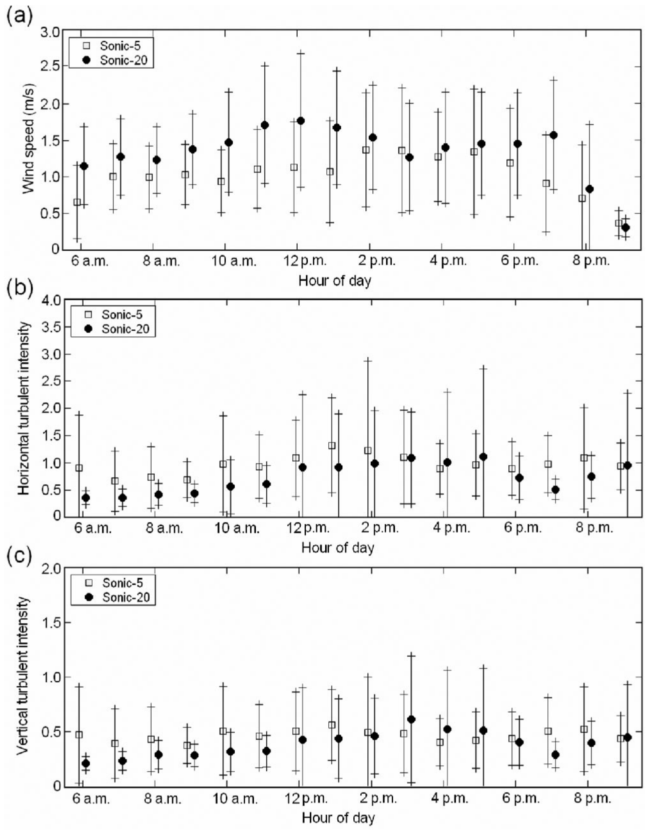

Figure 13. Variation in (a) wind speed, (b) horizontal, and (c) vertical turbulent intensities at 5 and 20 m from the road as a function of time of day.

NO PAC Reduction with Distance

The plume capture advantage offered by extended-path sampling facilitates investigations of parameters affecting the initial dispersion of the near-road emissions. For example, in this study, the reduction of NO concentrations from the 7- to 17-m observing locations can be estimated as a function of wind angle. Figure 14 shows the percentage reduction of NO PAC as a function of deviation of wind direction from the 206° normal vector. These data represent a grouped average of mean wind directions from 5:00 a.m. to 7:00 p.m. at half-hour time intervals

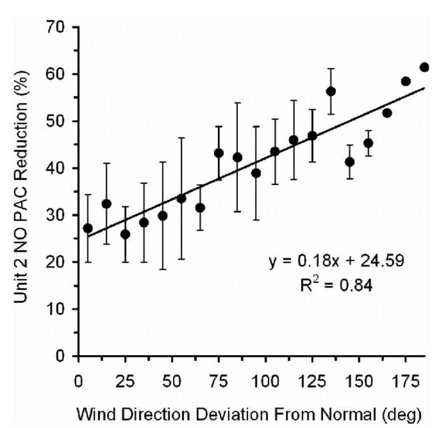

Figure 14. Unit 2 (17 m) NO PAC percentage reduction compared with unit 1 PAC (7 m) vs. wind direction deviation from normal.

binned in 10° increments. It is evident that the reduction in NO PAC between the 7- and 17-m locations increased when wind direction deviation from the normal direction increased. The regression intercept of Figure 14 indicates an approximate 25% reduction in NO PAC between the 7- and 17-m locations when winds were directly from the roadway. This agrees favorably with values from Fraigneau et al.[33] and Sahlodin et al.[34] on modeled concentration reductions of NO and CO, respectively; and additionally to measured CO reductions by Zhu et al.,[35] with the latter two based on the same study possessing a similar configuration to this study, having measurement points 4 and 17 m from road edge.

Because of the lack of comparable data with similar wind directions at different times of day, it was not possible to evaluate the effect of additional potential loss mechanisms such as increasing mixing height and ozone titration loss, which generally increase from morning through afternoon. Because of the quality of the correlations evident in Figure 12 ($R^2 = 0.84$), it can be argued that the aforementioned additional loss mechanisms have little effect on the time and spatial scales present in this study.

SUMMARY

The quantity, dispersion, and impact of motor vehicle emissions on near-roadway populations is an area of increasing importance. Because of its mobile source emission profile and low background concentration, NO is a useful tracer compound for investigating the initial dispersion parameters of roadway emissions. NO has clear source discrimination advantages compared with NO_2 for studies in close proximity to the road, especially for the important morning rush hour periods under crosswind conditions. This work demonstrated the use of DUV-DOAS systems deployed parallel to the road for robust capture and measurement of NO emissions. The path-integrated measurement approach coupled with three-dimensional wind measurements and traffic-monitoring data were shown to provide useful information on the parameters affecting near-road pollutant concentrations and on the initial stages of near-road dispersion. Near-road NO concentrations were shown to correlate with wind direction and traffic intensity. Significant NO concentrations were observed with winds away from the roadway and were ascribed to turbulent diffusion/meandering. The dilution of NO as a function of wind direction was also discussed. Future work will utilize this dataset to further parameterize emission and dispersion from this study.

ACKNOWLEDGMENTS

This work reflects the collaboration of many individuals working with EPA's near-road research program. In particular, the authors appreciate the direction and support of Dr. Dan Costa, EPA's National Program Director for Air, for leading the near-road research program and for funding assistance from EPA's Advanced Monitoring Initiative Grant. From EPA's Office of Research and Development, the authors also thank Edgar Thompson and Bill Mitchell for assistance in executing this effort, Sue Kimbrough and Bruce Harris for valuable discussions, and Jason Weinstein for assistance in project development and contract management for this study. The authors also thank Tom Long, Richard Snow, Eric Morris, Tom Balicki, and Dr. Ram Hashmonay of Arcadis for their work on the field study and for helpful discussions. Finally, the authors thank the North Carolina Lions Club for the Blind for access to portions of the field site used in this study.

Disclaimer: This article has been reviewed by EPA's Office of Research and Development and approved for publication. Approval does not signify that the contents necessarily reflect the views and policies of the agency nor does mention of trade names or commercial products constitute endorsement or recommendation for use. The research presented here was performed under the Memorandum of Understanding between EPA and the U.S. Department of Commerce's National Oceanic and Atmospheric Administration (NOAA) and under agreement number DW13921548. This work constitutes a contribution to the NOAA Air Quality Program. Although it has been reviewed by EPA and NOAA and approved for publication, it does not necessarily reflect their policies or views. The U.S. Government right to retain a nonexclusive royalty-free license in and to any copyright is acknowledged.

REFERENCES

1. U.S. Environmental Protection Agency. 2002 National Emission Inventory; available at *http://www.epa.gov/ttn/chief/net/2002inventory.html* (accessed March 12, 2007).
2. Brauer, M.; Hoek, G.; Van Vliet, P.; Meliefste, K.; Fishcer, P.H.; Wijga, A.; Koopman, L.P.; Neijens, H.J.; Gerritsen, J.; Kerkhof, M.; Heinrich, J.; Bellander, T.; Brunekreef, B. Air Pollution from Traffic and the Development of Respiratory Infections and Asthmatic and Allergic Symptoms in Children; *Am. J. Respir. Crit. Care Med.* **2002**, *166*, 1092-1098.
3. Brunekreef, B.; Janssen, N.A.; de Hartog, J.; Harssema, H.; Knape, M.; van Vliet, P. Air Pollution from Truck Traffic and Lung Function in Children Living near Motorways; *Epidemiol.* **1997**, *8*, 298-303.
4. Finkelstein, M.M.; Jerrett, M.; Sears, M.R. Traffic Air Pollution and Mortality Rate Advancement Periods; *Am. J. Epidemiol.* **2004**, *160,* 173-177.
5. Garshick, E.; Laden, F.; Hart, J.E.; Caron, A. Residence near a Major Road and Respiratory Symptoms in U.S. Veterans; *Epidemiol.* **2003**, *14*, 728-736.
6. Harrison, R.M.; Leung, P.L.; Somervaille, L. Analysis of Incidence of Childhood Cancer in the West Midlands of the United Kingdom in Relation to Proximity of Main Roads and Petrol Stations; *Occup. Environ. Med.* **1999**, *56,* 774-780.
7. Hoek, G.; Brunekreef, B.; Goldbohm, S.; Fischer, P.; van den Brandt, P.A. Association between Mortality and Indicators of Traffic-Related Air Pollution in the Netherlands: a Cohort Study; *Lancet* **2002**, *360*, 1203-1209.
8. Kim, J.J.; Smorodinsky, S.; Ostro, B.; Lipsett, M.; Singer, B.C.; Hogdson, A.T. Traffic-Related Air Pollution and Respiratory Health: the East Bay Children's Respiratory Health Study; *Epidemiol.* **2002**, *13*, S100.
9. McConnell, R.; Berhane, K.; Yao, L.; Jerrett, M.; Lurmann, F.; Gilliland, F.; Kuenzli, N.; Gauderman, J.; Avol, E.; Thomas, D.; Peters, J. Traffic, Susceptibility, and Childhood Asthma; *Environ. Health Perspect.* **2006**, *114*, 766-772.
10. Peters, A.; von Klot, S.; Heier, M.; Trentinaglia, I.; Hormann, A.; Wichmann, E.; Lowel, H. Exposure to Traffic and the Onset of Myocardial Infarction; *New Engl. J. Med.* **2004**, *351,* 1721-1730.
11. U.S. Census Bureau 2004 American Housing Survey, Table IA-6; available at *http://www.census.gov/hhes/www/housing/ahs/ahs03/ahs03.html* (accessed January 22, 2007).
12. Baldauf, R.; Thoma, E.; Hays, M.; Shores, R.; Kinsey, J.; Gullett, B.; Kimbrough, S.; Isakov, V.; Long, T.; Snow, R.; Khlystov, A.; Weinstein, J.; Chen, F.-L.; Seila, R.; Olson, D.; Gilmour, I.; Cho, S.-H.; Watkins, N.; Rowley, P.; Bang, J. Traffic and Meteorological Impacts on Near-Road Air Quality: Summary of Methods and Trends from the Raleigh Near-Road Study; *J. Air & Waste Manage. Assoc.* **2008,** *58,* 865-878.
13. Heywood, J.B. *Internal Combustion Engine Fundamentals*; McGraw-Hill: New York, 1988.
14. Atkinson, R. In *Air Pollution, The Automobile, and Public Health*; Watson, A.Y., Bates, R.R., Kennedy, D., Eds.; National Academy: Washington, DC, 1988; pp 99-132.

15. Janhäll, S.; Jonsson, A.M.; Molnár, P.; Svensson, E.A.; Hallquist, M.A. Size Resolved Traffic Emission Factors of Submicrometer Particles; *Atmos. Environ.* **2004**, *38,* 4331-4340.
16. *Optical Remote Sensing for Emission Characterization from Non-Point Sources*; EPA Test Method (OTM 10); U.S. Environmental Protection Agency Technology Transfer Network Emission Measurement Center, 2006; available at *http://www.epa.gov/ttn/emc/prelim.html* (accessed January 22, 2007).
17. Thoma, E.D.; Shores, R.C.; Thompson, E.L.; Harris, D.B.; Thorneloe, S.A.; Varma, R.M.; Hashmonay, R.A.; Modrak, M.T.; Natschke, D.F.; Gamble, H.A. Open Path Tunable Diode Laser Absorption Spectroscopy for Acquisition of Fugitive Emission Flux Data; *J. Air & Waste Manage. Assoc.* **2005**, *55,* 658-668.
18. Hashmonay, R.A.; Yost, M.G.; Mamane, Y.; Benayahu, Y. Emission Rate Apportionment from Fugitive Sources Using Open-Path FTIR and Mathematical Inversion; *Atmos. Environ.* **1999**, *33,* 735-743.
19. *Open-Path FTIR Compound Detection Limits*; Industrial Monitoring and Control: Round Rock, TX; available at *http://www.ftir.bz/limits.shtml* (accessed January 22, 2007).
20. Kuhns, H.D.; Mazzoleni, C.; Moosmüller, H.; Nikolic, D.; Keislar, R.E.; Barber, P.W.; Li, Z.; Etyemezian, V.; Watson, J.G. Remote Sensing of PM, NO, CO, and HC Emissions Factors for On-Road Gasoline and Diesel Engine Vehicles in Las Vegas, NV; *Sci. Tot. Environ.* **2004**, *322,* 123-137.
21. Bishop, G.A.; Burgard, D.A.; Stedman, D.H. *On-Road Remote Sensing of Automobile Emissions in the Chicago Area: Year 6, September 2004*; Report for Coordinating Research Council; Contract No. E-23-9, Project E-23-9, May 2006; available at *http://www.crcao.com/reports/recent_reports_and_study_results.htm* (accessed January 24, 2007).
22. Bishop, G.A.; Stedman, D.H.; Hutton, R.B.; Bohren, L.; Lacey, N. Drive-By Motor Vehicle Emissions: Immediate Feedback in Reducing Air Pollution; *Environ. Sci. Technol.* **2000**, *24,* 843-847.
23. Sjödin, A.; Andréasson, K. Multi-Year Remote-Sensing Measurements of Gasoline Light-Duty Vehicle Emissions on a Freeway Ramp; *Atmos. Environ.* **2000**, *34,* 4657-4665.
24. Popp, P.J.; Bishop, G.A.; Stedman, D.H. Development of a High-Speed Ultraviolet Spectrometer for Remote Sensing of Mobile Source Nitric Oxide Emissions; *J. Air & Waste Manage. Assoc.* **1999**, *49,* 1463-1468.
25. Platt, U. In *Air Monitoring by Spectroscopic Techniques*; Sigrist, M., Ed.; Wiley: New York, 1994; pp 27-84.
26. Kutter, W.; Lamp, T.; Weber, K. Summer Air Quality over an Artificial Lake; *Atmos. Environ.* **2002**, *36,* 5927-5936.
27. Schäfer, K.; Carsten, J.; Strum, P.; Lechner, B.; Bacher, M. Aircraft Emission: Measurement by Remote Sensing Methodologies at Airports; *Atmos. Environ.* **2003**, *37,* 5261-5271.
28. Pundt, I.; Mettendorf, K.-U.; Laepple, T.; Knab, V.; Xie, P.; Lösch, J.; Friedeburg, C.V.; Platt, U.; Wagner, T. Measurement of Trace Gas Distributions Using Long-Path DOAS-Tomography during the Motorway Campaign BABII: Experimental Setup and Results for NO_2; *Atmos. Environ.* **2005**, *39,* 967-975.
29. Kourtidis, K.A.; Ziomas, I.; Zerefos, C.; Kosmidis, E.; Symeonidis, P.; Christophilopoulos, E.; Karathanassis, S.; Mploutsos, A.; Benzene, Toluene, Ozone, NO_2, and SO_2, Measurements in an Urban Street Canyon in Thessaloniki, Greece; *Atmos. Environ.* **2002**, *36,* 5355-5364.
30. Thoma, E.D.; Thompson, E.L.; Shores, R.C.; Harris, D.B. Measurement of Low Level Air Toxics with Modified UV DOAS. In *Proceedings of the 99th Annual Conference of the Air & Waste Management Association*; A&WMA: Pittsburgh, PA, 2006; Paper AO-1b-270.
31. Vogt, F.; Klocke, U.; Schmidtke, G.; Wander, V.; Tacke, M. Optical UV Derivative Spectroscopy for Monitoring Gaseous Emissions; *Appl. Spectroscopy* **1999**, *53,* 1352-1360.
32. Isakov, V.; Sax, T.; Venkatram, A.; Pankratz, D.; Heumann, J.; Fitz, D. Near Field Dispersion Modeling for Regulatory Applications; *J. Air & Waste Manage. Assoc.* **2003**, *54,* 473-482.
33. Fraigneau, Y.C.; Gonzalez, M.; Copalle, A. Dispersion and Chemical Reaction of a Pollutant near a Motorway; *Sci. Tot. Environ.* **1995**, *169,* 83-91.
34. Sahlodin, A.M.; Sotudeh-Gharebagh, R.; Zhu; Y. Modeling of Dispersion near Roadways Based on Vehicle-Induced Turbulence Concept; *Atmos. Environ.* **2007**, *41,* 92-102.
35. Zhu, Y.; Hinds, W.C.; Kim, S.K.; Sioutas, C. Concentration and Size Distribution of Ultrafine Particles near a Major Highway; *J. Air & Waste Manage. Assoc.* **2002**, *52,* 1032-1042.

About the Authors

Eben Thoma, Richard Shores, and Rich Baldauf are scientists with EPA's Office of Research and Development, National Risk Management Research Laboratory in Research Triangle Park, NC. Rich Baldauf is additionally affiliated with EPA's Office of Air and Radiation, Office of Transportation and Air Quality, National Vehicle and Fuel Emissions Laboratory, in Ann Arbor, MI. Vlad Isakov is scientist with NOAA, Atmospheric Sciences Modeling Division, working in Partnership with EPA in Research Triangle Park, NC. Please address correspondence to: Eben Thoma, 109 TW Alexander Drive, E343-02, Research Triangle Park, NC 27711; phone: +1-919-541-7969; fax: +1-919-541-0359; e-mail: thoma.eben@epa.gov.